

NNLO QCD Corrections to the $\bar{B} \rightarrow X_s \gamma$ Matrix Elements Using Interpolation in m_c

Mikołaj Misiak^{1,2} and Matthias Steinhauser³

¹ *Institute of Theoretical Physics, Warsaw University,
Hoża 69, PL-00-681 Warsaw, Poland.*

² *Theoretical Physics Division, CERN, CH-1211 Geneva 23, Switzerland.*

³ *Institut für Theoretische Teilchenphysik, Universität Karlsruhe (TH),
D-76128 Karlsruhe, Germany.*

Abstract

One of the most troublesome contributions to the NNLO QCD corrections to $\bar{B} \rightarrow X_s \gamma$ originates from three-loop matrix elements of four-quark operators. A part of this contribution that is proportional to the QCD beta-function coefficient β_0 was found in 2003 as an expansion in m_c/m_b . In the present paper, we evaluate the asymptotic behaviour of the complete contribution for $m_c \gg m_b/2$. The asymptotic form of the β_0 -part matches the small- m_c expansion very well at the threshold $m_c = m_b/2$. For the remaining part, we perform an interpolation down to the measured value of m_c , assuming that the β_0 -part is a good approximation at $m_c = 0$. Combining our results with other contributions to the NNLO QCD corrections, we find $\mathcal{B}(\bar{B} \rightarrow X_s \gamma) = (3.15 \pm 0.23) \times 10^{-4}$ for $E_\gamma > 1.6$ GeV in the \bar{B} -meson rest frame. The indicated error has been obtained by adding in quadrature the following uncertainties: non-perturbative (5%), parametric (3%), higher-order perturbative (3%), and the interpolation ambiguity (3%).

1 Introduction

The decay $\bar{B} \rightarrow X_s \gamma$ is a well-known probe of new physics at the electroweak scale. The current world average for its branching ratio with a cut $E_\gamma > 1.6$ GeV in the \bar{B} -meson rest frame reads [1]

$$\mathcal{B}(\bar{B} \rightarrow X_s \gamma)_{E_\gamma > 1.6 \text{ GeV}}^{\text{exp}} = (3.55 \pm 0.24 \text{ }^{+0.09}_{-0.10} \pm 0.03) \times 10^{-4}, \quad (1.1)$$

where the first error is combined statistical and systematic. The second one is due to the theory input on the shape function. The third one is caused by the $b \rightarrow d \gamma$ contamination.

The total error in Eq. (1.1) amounts to around 7.4%, i.e. it is of the same size as the expected $\mathcal{O}(\alpha_s^2)$ corrections to the perturbative transition $b \rightarrow X_s^{\text{parton}} \gamma$. On the other hand, the relation

$$\Gamma(\bar{B} \rightarrow X_s \gamma) \simeq \Gamma(b \rightarrow X_s^{\text{parton}} \gamma) \quad (1.2)$$

holds up to non-perturbative corrections that turn out to be smaller (see Section 7). Consequently, evaluating the Next-to-Next-to-Leading Order (NNLO) QCD corrections to $b \rightarrow X_s^{\text{parton}} \gamma$ is of crucial importance for deriving constraints on new physics from the measurements of $\bar{B} \rightarrow X_s \gamma$.

In the calculation of $b \rightarrow X_s^{\text{parton}} \gamma$, resummation of large logarithms $(\alpha_s \ln M_W^2/m_b^2)^n$ is necessary at each order in α_s , which is most conveniently performed in the framework of an effective theory that arises from the Standard Model (SM) after decoupling the heavy electroweak bosons and the top quark. The explicit form of the relevant effective Lagrangian is given in the next section. The Wilson coefficients $C_i(\mu)$ play the role of coupling constants at the flavour-changing vertices (operators) Q_i .

The perturbative calculations are performed in three steps:

- (i) Matching: Evaluating $C_i(\mu_0)$ at the renormalization scale $\mu_0 \sim M_W, m_t$ by requiring equality of the SM and effective theory Green's functions at the leading order in (external momenta)/(M_W, m_t).
- (ii) Mixing: Calculating the operator mixing under renormalization, deriving the effective theory Renormalization Group Equations (RGE) and evolving $C_i(\mu)$ from μ_0 down to the low-energy scale $\mu_b \sim m_b$.
- (iii) Matrix elements: Evaluating the on-shell $b \rightarrow X_s^{\text{parton}} \gamma$ amplitudes at $\mu_b \sim m_b$.

In the NNLO analysis of the considered decay, the four-quark operators Q_1, \dots, Q_6 and the dipole operators Q_7 and Q_8 must be matched at the two- and three-loop level, respectively. Three-point amplitudes with four-quark vertices need to be renormalized up to the four-loop level, while “only” three-loop mixing is necessary in the remaining cases. The matrix elements are needed up to two loops for the dipole operators, and up to three loops for the four-quark operators.

The NNLO matching was calculated in Refs. [2, 3]. The three-loop renormalization in the $\{Q_1, \dots, Q_6\}$ and $\{Q_7, Q_8\}$ sectors was found in Refs. [4, 5]. The results from Ref. [6] on the four-loop mixing of Q_1, \dots, Q_6 into Q_7 will be used in our numerical analysis.¹

¹ The small effect (−0.35% in the branching ratio) of the four-loop mixing [6] of Q_1, \dots, Q_6 into Q_8 is neglected here. It was not yet known in September 2006 when the current paper was being completed.

As far as the matrix elements are concerned, contributions to the decay rate that are proportional to $|C_7(\mu_b)|^2$ are completely known at the NNLO thanks to the calculations in Refs. [7, 8]. These two-loop results have recently been confirmed by an independent group [9, 10]. Two- and three-loop matrix elements in the so-called large- β_0 approximation were found in Ref. [11] as expansions in the quark mass ratio m_c/m_b . Such expansions are adequate when $m_c < m_b/2$, which is satisfied by the measured quark masses. Finding all the remaining (“beyond- β_0 ”) contributions to the matrix elements is a very difficult task because hundreds of massive three-loop on-shell vertex diagrams need to be calculated.

In the present work, we evaluate the asymptotic form of the m_c -dependent NNLO matrix elements in the limit $m_c \gg m_b/2$ using the same decoupling technique as in our three-loop Wilson coefficient calculation [3]. We find that the asymptotic form of the β_0 -part matches the small- m_c expansion very well at the $c\bar{c}$ production threshold $m_c = m_b/2$. The same is true for the Next-to-Leading Order (NLO) matrix elements. Motivated by this observation, we interpolate the beyond- β_0 part to smaller values of m_c assuming that the β_0 -part is a good approximation at $m_c = 0$. Combining our results with other contributions to the NNLO QCD corrections, we find an estimate for the branching ratio at $\mathcal{O}(\alpha_s^2)$.

Our paper is organized as follows. In Section 2, we introduce the effective theory and collect the relevant formulae for the $\bar{B} \rightarrow X_s \gamma$ branching ratio. The contributions that are known exactly in m_c are described in Section 3. Expressions for the NNLO matrix elements in the large- β_0 approximation and in the $m_c \gg m_b/2$ limit are presented in Sections 4 and 5, respectively. Section 6 is devoted to discussing the interpolation in m_c . Section 7 contains the analysis of uncertainties. We conclude in Section 8. Our numerical input parameters are collected in Appendix A. Appendix B contains a discussion of the $c\bar{c}$ production treatment in the interpolation.

2 The effective theory

Following Section 3 of Ref. [12], the $\bar{B} \rightarrow X_s \gamma$ branching ratio can be expressed as follows:

$$\mathcal{B}[\bar{B} \rightarrow X_s \gamma]_{E_\gamma > E_0} = \mathcal{B}[\bar{B} \rightarrow X_c e \bar{\nu}]_{\text{exp}} \left| \frac{V_{ts}^* V_{tb}}{V_{cb}} \right|^2 \frac{6\alpha_{\text{em}}}{\pi C} [P(E_0) + N(E_0)], \quad (2.1)$$

where $\alpha_{\text{em}} = \alpha_{\text{em}}(0) \simeq 1/137.036$ and $N(E_0)$ denotes the non-perturbative correction.² The m_c -dependence of $\bar{B} \rightarrow X_c e \bar{\nu}$ is accounted for by

$$C = \left| \frac{V_{ub}}{V_{cb}} \right|^2 \frac{\Gamma[\bar{B} \rightarrow X_c e \bar{\nu}]}{\Gamma[\bar{B} \rightarrow X_u e \bar{\nu}]}, \quad (2.2)$$

with neglected spectator annihilation. $P(E_0)$ is given by the perturbative ratio

$$\frac{\Gamma[b \rightarrow X_s \gamma]_{E_\gamma > E_0}}{|V_{cb}/V_{ub}|^2 \Gamma[b \rightarrow X_u e \bar{\nu}]} = \left| \frac{V_{ts}^* V_{tb}}{V_{cb}} \right|^2 \frac{6\alpha_{\text{em}}}{\pi} P(E_0). \quad (2.3)$$

² See Eqs. (3.10) and (4.7) of Ref. [12]. The corrections found in Eqs. (3.9) and (3.14) of Ref. [13] as well as Eq. (28) of Ref. [14] should be included in $N(E_0)$, too.

Our goal is to calculate the NNLO QCD corrections to the quantity $P(E_0)$. The denominator on the l.h.s. of Eq. (2.3) is already known at the NNLO level from Refs. [15, 16].

The relevant effective Lagrangian reads

$$\mathcal{L}_{\text{eff}} = \mathcal{L}_{\text{QCD} \times \text{QED}}(u, d, s, c, b) + \frac{4G_F}{\sqrt{2}} \left[V_{ts}^* V_{tb} \sum_{i=1}^8 C_i Q_i + V_{us}^* V_{ub} \sum_{i=1}^2 C_i^c (Q_i^u - Q_i) \right], \quad (2.4)$$

where

$$\begin{aligned} Q_1^u &= (\bar{s}_L \gamma_\mu T^a u_L)(\bar{u}_L \gamma^\mu T^a b_L), \\ Q_2^u &= (\bar{s}_L \gamma_\mu u_L)(\bar{u}_L \gamma^\mu b_L), \\ Q_1 &= (\bar{s}_L \gamma_\mu T^a c_L)(\bar{c}_L \gamma^\mu T^a b_L), \\ Q_2 &= (\bar{s}_L \gamma_\mu c_L)(\bar{c}_L \gamma^\mu b_L), \\ Q_3 &= (\bar{s}_L \gamma_\mu b_L) \sum_q (\bar{q} \gamma^\mu q), \\ Q_4 &= (\bar{s}_L \gamma_\mu T^a b_L) \sum_q (\bar{q} \gamma^\mu T^a q), \\ Q_5 &= (\bar{s}_L \gamma_{\mu_1} \gamma_{\mu_2} \gamma_{\mu_3} b_L) \sum_q (\bar{q} \gamma^{\mu_1} \gamma^{\mu_2} \gamma^{\mu_3} q), \\ Q_6 &= (\bar{s}_L \gamma_{\mu_1} \gamma_{\mu_2} \gamma_{\mu_3} T^a b_L) \sum_q (\bar{q} \gamma^{\mu_1} \gamma^{\mu_2} \gamma^{\mu_3} T^a q), \\ Q_7 &= \frac{e}{16\pi^2} m_b (\bar{s}_L \sigma^{\mu\nu} b_R) F_{\mu\nu}, \\ Q_8 &= \frac{g}{16\pi^2} m_b (\bar{s}_L \sigma^{\mu\nu} T^a b_R) G_{\mu\nu}^a. \end{aligned} \quad (2.5)$$

The last term in the square bracket of Eq. (2.4) gives no contribution at the Leading Order (LO) and only a small contribution at the NLO (around +1% in the branching ratio — see Eq. (3.7) of Ref. [12]). Consequently, we shall neglect its effect on the NNLO QCD correction and omit terms proportional to V_{ub} in the analytical formulae below. However, our numerical results will include the V_{ub} terms at the NLO. The same refers to the electroweak corrections that amount to around −3.7% in $P(E_0)$ [12, 17].

The quantity $P(E_0)$ depends quadratically on the Wilson coefficients³

$$P(E_0) = \sum_{i,j=1}^8 C_i^{\text{eff}}(\mu_b) C_j^{\text{eff}}(\mu_b) K_{ij}(E_0, \mu_b), \quad (2.6)$$

where the “effective coefficients” are defined by

$$C_i^{\text{eff}}(\mu) = \begin{cases} C_i(\mu), & \text{for } i = 1, \dots, 6, \\ C_7(\mu) + \sum_{j=1}^6 y_j C_j(\mu), & \text{for } i = 7, \\ C_8(\mu) + \sum_{j=1}^6 z_j C_j(\mu), & \text{for } i = 8. \end{cases} \quad (2.7)$$

The numbers y_j and z_j are defined so that the leading-order $b \rightarrow s\gamma$ and $b \rightarrow sg$ matrix elements of the effective Hamiltonian are proportional to the leading-order terms in C_7^{eff} and C_8^{eff} , respectively [18]. This means, in particular, that $K_{ij} = \delta_{i7}\delta_{j7} + \mathcal{O}(\alpha_s)$. In the $\overline{\text{MS}}$ scheme with fully anticommuting γ_5 , $\vec{y} = (0, 0, -\frac{1}{3}, -\frac{4}{9}, -\frac{20}{3}, -\frac{80}{9})$ and $\vec{z} = (0, 0, 1, -\frac{1}{6}, 20, -\frac{10}{3})$ [19].

³ In Eq. (30) of Ref. [7], K_{ij} was denoted by \tilde{G}_{ij}/G_u .

In Eq. (2.6), we have assumed that all the Wilson coefficients are real, as it is the case in the SM. Consequently, K_{ij} is a real symmetric matrix.

Once the $\overline{\text{MS}}$ -renormalized⁴ coefficients $C_i^{\text{eff}}(\mu)$ are perturbatively expanded

$$C_i^{\text{eff}}(\mu) = C_i^{(0)\text{eff}}(\mu) + \tilde{\alpha}_s(\mu)C_i^{(1)\text{eff}}(\mu) + \tilde{\alpha}_s^2(\mu)C_i^{(2)\text{eff}}(\mu) + \mathcal{O}(\tilde{\alpha}_s^3(\mu)), \quad (2.8)$$

where

$$\tilde{\alpha}_s(\mu_b) \equiv \frac{\alpha_s^{(5)}(\mu_b)}{4\pi}, \quad (2.9)$$

the expression for $P(E_0)$ can be cast in the following form:

$$\begin{aligned} P(E_0) &= P^{(0)}(\mu_b) + \tilde{\alpha}_s(\mu_b) \left[P_1^{(1)}(\mu_b) + P_2^{(1)}(E_0, \mu_b) \right] \\ &+ \tilde{\alpha}_s^2(\mu_b) \left[P_1^{(2)}(\mu_b) + P_2^{(2)}(E_0, \mu_b) + P_3^{(2)}(E_0, \mu_b) \right] + \mathcal{O}(\tilde{\alpha}_s^3(\mu_b)). \end{aligned} \quad (2.10)$$

Here, $P^{(0)}$ and $P_1^{(k)}$ originate from the tree-level matrix element of Q_7

$$\begin{aligned} P^{(0)}(\mu_b) &= \left(C_7^{(0)\text{eff}}(\mu_b) \right)^2, \\ P_1^{(1)}(\mu_b) &= 2C_7^{(0)\text{eff}}(\mu_b)C_7^{(1)\text{eff}}(\mu_b), \\ P_1^{(2)}(\mu_b) &= \left(C_7^{(1)\text{eff}}(\mu_b) \right)^2 + 2C_7^{(0)\text{eff}}(\mu_b)C_7^{(2)\text{eff}}(\mu_b), \end{aligned} \quad (2.11)$$

while $P_2^{(k)}$ depend only on the LO Wilson coefficients $C_i^{(0)\text{eff}}$. The NNLO correction $P_3^{(2)}$ is defined by requiring that it is proportional to products of the LO and NLO Wilson coefficients only ($C_i^{(0)\text{eff}}C_j^{(1)\text{eff}}$).

3 The corrections $P_2^{(1)}$ and $P_3^{(2)}$

The corrections $P_2^{(1)}$ and $P_3^{(2)}$ are known exactly in m_c . In order to describe their content, we expand $K_{ij}(E_0, \mu_b)$ in $\tilde{\alpha}_s(\mu_b)$

$$K_{ij} = \delta_{i7}\delta_{j7} + \tilde{\alpha}_s(\mu_b)K_{ij}^{(1)} + \tilde{\alpha}_s^2(\mu_b)K_{ij}^{(2)} + \mathcal{O}(\tilde{\alpha}_s^3(\mu_b)). \quad (3.1)$$

The coefficients $K_{ij}^{(1)}$ are easily derived from the known NLO results

$$K_{i7}^{(1)} = \text{Re } r_i^{(1)} - \frac{1}{2}\gamma_{i7}^{(0)\text{eff}}L_b + 2\phi_{i7}^{(1)}(\delta), \quad \text{for } i \leq 6, \quad (3.2)$$

$$K_{77}^{(1)} = -\frac{182}{9} + \frac{8}{9}\pi^2 - \gamma_{77}^{(0)\text{eff}}L_b + 4\phi_{77}^{(1)}(\delta), \quad (3.3)$$

$$K_{78}^{(1)} = \frac{44}{9} - \frac{8}{27}\pi^2 - \frac{1}{2}\gamma_{87}^{(0)\text{eff}}L_b + 2\phi_{78}^{(1)}(\delta), \quad (3.4)$$

$$K_{ij}^{(1)} = 2(1 + \delta_{ij})\phi_{ij}^{(1)}(\delta), \quad \text{for } i, j \neq 7, \quad (3.5)$$

⁴ The evanescent operators are as in Eqs. (23)–(25) of Ref. [4].

where

$$L_b = \ln \left(\frac{\mu_b}{m_b^{1S}} \right)^2. \quad (3.6)$$

The matrix $\hat{\gamma}^{(0)\text{eff}}$ and the quantities $r_i^{(1)}$ as functions of

$$z = \left(\frac{m_c(\mu_c)}{m_b^{1S}} \right)^2 \quad (3.7)$$

can be found respectively in Eqs. (6.3) and (3.1) of Ref. [20]. The bottom mass is renormalized in the $1S$ scheme [21] throughout the paper. The charm mass $\overline{\text{MS}}$ renormalization scale μ_c is chosen to be independent from μ_b . For future convenience, we quote $r_{1,2}^{(1)}$:

$$r_2^{(1)}(z) = -6 r_1^{(1)}(z) = -\frac{1666}{243} + 2[a(z) + b(z)] - \frac{80}{81}i\pi. \quad (3.8)$$

The exact expressions for $a(z)$ and $b(z)$ in terms of Feynman parameter integrals can be found in Eqs. (3.3) and (3.4) of Ref. [20]. Their small- m_c expansions up to $\mathcal{O}(z^4)$ read [22, 23]

$$\begin{aligned} a(z) = & \frac{16}{9} \left\{ \left[\frac{5}{2} - \frac{\pi^2}{3} - 3\zeta(3) + \left(\frac{5}{2} - \frac{3\pi^2}{4} \right) L_z + \frac{1}{4}L_z^2 + \frac{1}{12}L_z^3 \right] z + \left(\frac{7}{4} + \frac{2\pi^2}{3} - \frac{\pi^2}{2}L_z \right. \right. \\ & - \left. \frac{1}{4}L_z^2 + \frac{1}{12}L_z^3 \right) z^2 + \left[-\frac{7}{6} - \frac{\pi^2}{4} + 2L_z - \frac{3}{4}L_z^2 \right] z^3 + \left(\frac{457}{216} - \frac{5\pi^2}{18} - \frac{1}{72}L_z - \frac{5}{6}L_z^2 \right) z^4 \\ & + \left. i\pi \left[\left(4 - \frac{\pi^2}{3} + L_z + L_z^2 \right) \frac{z}{2} + \left(\frac{1}{2} - \frac{\pi^2}{6} - L_z + \frac{1}{2}L_z^2 \right) z^2 + z^3 + \frac{5}{9}z^4 \right] \right\} + \mathcal{O}(z^5 L_z^2), \end{aligned} \quad (3.9)$$

$$\begin{aligned} b(z) = & -\frac{8}{9} \left\{ \left(-3 + \frac{\pi^2}{6} - L_z \right) z - \frac{2\pi^2}{3} z^{3/2} + \left(\frac{1}{2} + \pi^2 - 2L_z - \frac{1}{2}L_z^2 \right) z^2 \right. \\ & + \left(-\frac{25}{12} - \frac{1}{9}\pi^2 - \frac{19}{18}L_z + 2L_z^2 \right) z^3 + \left(-\frac{1376}{225} + \frac{137}{30}L_z + 2L_z^2 + \frac{2\pi^2}{3} \right) z^4 \\ & + \left. i\pi \left[-z + (1 - 2L_z)z^2 + \left(-\frac{10}{9} + \frac{4}{3}L_z \right) z^3 + z^4 \right] \right\} + \mathcal{O}(z^5 L_z^2), \end{aligned} \quad (3.10)$$

where

$$L_z = \ln z. \quad (3.11)$$

The functions $\phi_{ij}^{(1)}(\delta \equiv 1 - 2E_0/m_b^{1S})$ with $i, j \in \{1, 2, 7, 8\}$ can be found in Appendix E of Ref. [12]. The remaining ones (that affect $P(1.6 \text{ GeV})$ by $\sim 0.1\%$ only) can be read out from the results of Ref. [24]. In particular,

$$\phi_{47}^{(1)}(\delta) = -\frac{1}{54}\delta \left(1 - \delta + \frac{1}{3}\delta^2 \right) + \frac{1}{12} \lim_{m_c \rightarrow m_b} \phi_{27}^{(1)}(\delta), \quad (3.12)$$

$$\phi_{48}^{(1)}(\delta) = -\frac{1}{3}\phi_{47}^{(1)}(\delta). \quad (3.13)$$

Once all the ingredients of $K_{ij}^{(1)}$ have been specified, $P_2^{(1)}$ and $P_3^{(2)}$ are evaluated by simple substitutions to Eq. (2.6)

$$P_2^{(1)} = \sum_{i,j=1}^8 C_i^{(0)\text{eff}} C_j^{(0)\text{eff}} K_{ij}^{(1)}, \quad (3.14)$$

$$P_3^{(2)} = 2 \sum_{i,j=1}^8 C_i^{(0)\text{eff}} C_j^{(1)\text{eff}} K_{ij}^{(1)}. \quad (3.15)$$

4 The β_0 -part of $P_2^{(2)}$

The only NNLO correction to $P(E_0)$ in Eq. (2.10) that has not yet been given is $P_2^{(2)}$. For this contribution, we shall neglect the tiny LO Wilson coefficients of Q_3, \dots, Q_6 . The NLO matrix elements of these operators affect the branching ratio by only around 1% [20]. Thus, neglecting the corresponding NNLO ones has practically no influence on the final accuracy.

Let us split $K_{ij}^{(2)}$ into the β_0 -parts $K_{ij}^{(2)\beta_0}$ and the remaining parts $K_{ij}^{(2)\text{rem}}$

$$K_{ij}^{(2)} = A_{ij} n_f + B_{ij} = K_{ij}^{(2)\beta_0} + K_{ij}^{(2)\text{rem}}, \quad (4.1)$$

where n_f stands for the number of massless flavours in the effective theory, and

$$K_{ij}^{(2)\beta_0} \equiv -\frac{3}{2}\beta_0 A_{ij} = -\frac{3}{2} \left(11 - \frac{2}{3}n_f \right) A_{ij}, \quad K_{ij}^{(2)\text{rem}} \equiv \frac{33}{2}A_{ij} + B_{ij}. \quad (4.2)$$

Following Ref. [11], we shall take $n_f = 5$. Effects related to the absence of real $c\bar{c}$ production in $b \rightarrow X_s^{\text{parton}}\gamma$ and to non-zero masses in quark loops on gluon propagators are relegated to $K_{ij}^{(2)\text{rem}}$. Thus, the only m_c -dependent contributions to $K_{ij}^{(2)\beta_0}$ originate from charm loops containing the four-quark vertices Q_1 and Q_2 .

The explicit $K_{ij}^{(2)\beta_0}$ that we derive from the results of Refs. [7, 8, 11, 15, 20] read

$$K_{27}^{(2)\beta_0} = \beta_0 \text{Re} \left\{ -\frac{3}{2}r_2^{(2)}(z) + 2 \left[a(z) + b(z) - \frac{290}{81} \right] L_b - \frac{100}{81}L_b^2 \right\} + 2\phi_{27}^{(2)\beta_0}(\delta), \quad (4.3)$$

$$K_{17}^{(2)\beta_0} = -\frac{1}{6}K_{27}^{(2)\beta_0}, \quad (4.4)$$

$$K_{77}^{(2)\beta_0} = \beta_0 \left\{ -\frac{3803}{54} - \frac{46}{27}\pi^2 + \frac{80}{3}\zeta(3) + \left(\frac{8}{9}\pi^2 - \frac{98}{3} \right) L_b - \frac{16}{3}L_b^2 \right\} + 4\phi_{77}^{(2)\beta_0}(\delta), \quad (4.5)$$

$$K_{78}^{(2)\beta_0} = \beta_0 \left\{ \frac{1256}{81} - \frac{64}{81}\pi^2 - \frac{32}{9}\zeta(3) + \left(\frac{188}{27} - \frac{8}{27}\pi^2 \right) L_b + \frac{8}{9}L_b^2 \right\} + 2\phi_{78}^{(2)\beta_0}(\delta), \quad (4.6)$$

$$K_{ij}^{(2)\beta_0} = 2(1 + \delta_{ij})\phi_{ij}^{(2)\beta_0}(\delta), \quad \text{for } i, j \neq 7. \quad (4.7)$$

The small- m_c expansion of $\text{Re } r_2^{(2)}(z)$ up to $\mathcal{O}(z^4)$ was calculated by Bieri *et al.* [11]

$$\text{Re } r_2^{(2)}(z) = \frac{67454}{6561} - \frac{124\pi^2}{729} - \frac{4}{1215} \left(11280 - 1520\pi^2 - 171\pi^4 - 5760\zeta(3) + 6840L_z \right)$$

$$\begin{aligned}
& - 1440\pi^2 L_z - 2520\zeta(3)L_z + 120L_z^2 + 100L_z^3 - 30L_z^4) z \\
& - \frac{64\pi^2}{243} (43 - 12 \ln 2 - 3L_z) z^{3/2} - \frac{2}{1215} (11475 - 380\pi^2 + 96\pi^4 + 7200\zeta(3) \\
& - 1110L_z - 1560\pi^2 L_z + 1440\zeta(3)L_z + 990L_z^2 + 260L_z^3 - 60L_z^4) z^2 \\
& + \frac{2240\pi^2}{243} z^{5/2} - \frac{2}{2187} (62471 - 2424\pi^2 - 33264\zeta(3) - 19494L_z - 504\pi^2 L_z \\
& - 5184L_z^2 + 2160L_z^3) z^3 - \frac{2464}{6075} \pi^2 z^{7/2} + \left(-\frac{15103841}{546750} + \frac{7912}{3645} \pi^2 + \frac{2368}{81} \zeta(3) \right. \\
& \left. + \frac{147038}{6075} L_z + \frac{352}{243} \pi^2 L_z + \frac{88}{243} L_z^2 - \frac{512}{243} L_z^3 \right) z^4 + \mathcal{O}(z^{9/2} L_z^4). \tag{4.8}
\end{aligned}$$

The function $\phi_{77}^{(2)\beta_0}(\delta)$ reads

$$\phi_{77}^{(2)\beta_0}(\delta) = \beta_0 \left[\phi_{77}^{(1)}(\delta) L_b + 4 \int_0^{1-\delta} dx F^{(2,nf)} \right], \tag{4.9}$$

where $F^{(2,nf)}$ as a function of $x = 2E_\gamma/m_b$ is given in Eq. (9) of Ref. [8].⁵

The remaining functions $\phi_{ij}^{(2)\beta_0}(\delta)$ will be neglected in our numerical analysis. It should not cause any significant uncertainty for $E_0 = 1.6 \text{ GeV}$. For this particular cut, the NLO functions $\phi_{ij}^{(1)}(\delta)$ affect the branching ratio by around -4% only, which is partly due to a certain convention in their definitions ($\phi_{ij}^{(1)}(0) = 0$ for $(ij) \neq (77)$, and $\phi_{77}^{(1)}(1) = 0$). An analogous convention is used for $\phi_{ij}^{(2)\beta_0}(\delta)$. The known $\phi_{77}^{(2)\beta_0}(\delta)$ affects the branching ratio by around -0.4% only. If the NLO pattern is repeated, an effect of similar magnitude is expected from the other $\phi_{ij}^{(2)\beta_0}(\delta)$.

As in Eq. (4.1), we can split $P_2^{(2)} = P_2^{(2)\beta_0} + P_2^{(2)\text{rem}}$ and express $P_2^{(2)\beta_0}$ in terms of $K_{ij}^{(2)\beta_0}$, by analogy to Eq. (3.14)

$$P_2^{(2)\beta_0} \simeq \sum_{i,j=1,2,7,8} C_i^{(0)\text{eff}} C_j^{(0)\text{eff}} K_{ij}^{(2)\beta_0}. \tag{4.10}$$

The “ \simeq ” sign is used above only because we skip $i, j = 3, 4, 5, 6$ in the sum.

5 The full correction $P_2^{(2)}$ in the limit $m_c \gg m_b/2$

The present section contains the main new result of our paper, namely the asymptotic form of $P_2^{(2)}$ in the limit $m_c \gg m_b/2$. It has been evaluated by performing a formal three-loop decoupling of the charm quark in the effective theory, using the method that has been previously applied by us to the calculation of the three-loop matching at the electroweak scale [3, 25]. Once the charm decoupling scale is set equal to μ_b , one recovers the asymptotic form of the matrix elements in the large m_c limit. Details of this calculation will be presented elsewhere [26].

⁵ The original calculation of $F^{(2,nf)}$ and several other contributions to the photon spectrum was performed in Ref. [27].

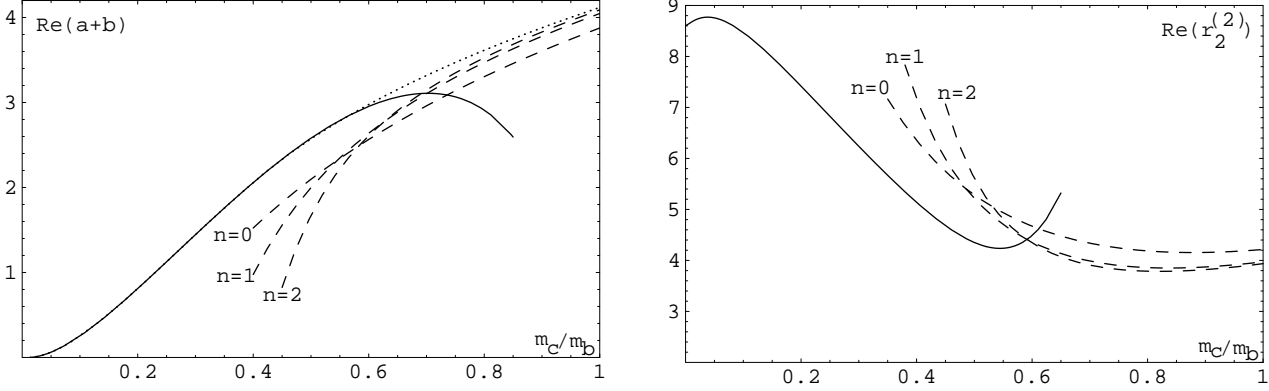


Figure 1: $\text{Re}(a+b)$ (left plot) and $\text{Re} r_2^{(2)}$ (right plot) as functions of $m_c/m_b = \sqrt{z}$. See the text for explanation of the curves.

The m_c -dependence of $P(E_0)$ at the NLO is dominated by $\text{Re}[a(z) + b(z)]$. At the two-loop level, we find the following asymptotic form of the functions $a(z)$ and $b(z)$

$$\text{Re} a(z) = \frac{4}{3}L_z + \frac{34}{9} + \frac{1}{z} \left(\frac{5}{27}L_z + \frac{101}{486} \right) + \frac{1}{z^2} \left(\frac{1}{15}L_z + \frac{1393}{24300} \right) + \mathcal{O}\left(\frac{1}{z^3}\right), \quad (5.1)$$

$$\text{Re} b(z) = -\frac{4}{81}L_z + \frac{8}{81} - \frac{1}{z} \left(\frac{2}{45}L_z + \frac{76}{2025} \right) - \frac{1}{z^2} \left(\frac{4}{189}L_z + \frac{487}{33075} \right) + \mathcal{O}\left(\frac{1}{z^3}\right). \quad (5.2)$$

$\text{Im} a(z) = \frac{4}{9}i\pi$ and $\text{Im} b(z) = \frac{4}{81}i\pi$ are exactly constant for $z > \frac{1}{4}$.

For the real part of the three-loop function $r_2^{(2)}(z)$ introduced in Eq. (4.3), we find

$$\begin{aligned} \text{Re} r_2^{(2)}(z) &= \frac{8}{9}L_z^2 + \frac{112}{243}L_z + \frac{27650}{6561} + \frac{1}{z} \left(\frac{38}{405}L_z^2 - \frac{572}{18225}L_z + \frac{10427}{30375} - \frac{8}{135}\pi^2 \right) \\ &+ \frac{1}{z^2} \left(\frac{86}{2835}L_z^2 - \frac{1628}{893025}L_z + \frac{19899293}{125023500} - \frac{8}{405}\pi^2 \right) + \mathcal{O}\left(\frac{1}{z^3}\right). \end{aligned} \quad (5.3)$$

The small- m_c expansion of this function has been given in Eq. (4.8).

The dotted line in the left plot of Fig. 1 corresponds to the exact expression for $\text{Re}(a+b)$. The solid line presents its small- m_c expansion up to $\mathcal{O}(z^4)$. The dashed lines are found from the large- m_c expansion including terms up to $\mathcal{O}(z^{-n})$ with $n = 0, 1, 2$, which is indicated by labels at the curves. The solid and dashed lines in the right plot of Fig. 1 present the same expansions of $\text{Re} r_2^{(2)}$. No exact expression is known in this case.

The plots in Fig. 1 clearly demonstrate that a combination of the small- m_c expansion for $m_c < m_b/2$ and the large- m_c expansion for $m_c > m_b/2$ (even in the $n = 0$ case) leads to a reasonable approximation to $\text{Re}(a+b)$ and $\text{Re} r_2^{(2)}$ for any m_c . Moreover, no large $c\bar{c}$ threshold effects are seen at $m_c = m_b/2$. These observations motivate us to calculate the $n = 0$ term in the large- m_c expansion of $P_2^{(2)\text{rem}}$ and use it in Section 6 to estimate this quantity for $m_c < m_b/2$.

The expressions that we have found for the leading terms in the large- m_c expansion of $K_{ij}^{(2)\text{rem}}$ are presented below. The necessary leading terms of $K_{ij}^{(1)}$ are easily derived from Eqs. (5.1)

and (5.2), taking into account that only $\phi_{ij}^{(1)}$ with $i, j > 2$ do not vanish at large z , and that $\phi_{ij}^{(1)}$ are z -independent for $i, j = 4, 7, 8$.

$$\begin{aligned} K_{22}^{(2)\text{rem}} &= 36 K_{11}^{(2)\text{rem}} + \mathcal{O}\left(\frac{1}{z}\right) = -6 K_{12}^{(2)\text{rem}} + \mathcal{O}\left(\frac{1}{z}\right) = \left(K_{27}^{(1)}\right)^2 + \mathcal{O}\left(\frac{1}{z}\right) \\ &= \left[\frac{218}{243} - \frac{208}{81}L_D\right]^2 + \mathcal{O}\left(\frac{1}{z}\right), \end{aligned} \quad (5.4)$$

$$\begin{aligned} K_{27}^{(2)\text{rem}} &= K_{27}^{(1)} K_{77}^{(1)} + \left(\frac{127}{324} - \frac{35}{27}L_D\right) K_{78}^{(1)} + \frac{2}{3}(1 - L_D)K_{47}^{(1)\text{rem}} \\ &\quad - \frac{4736}{729}L_D^2 + \frac{1150}{729}L_D - \frac{1617980}{19683} + \frac{20060}{243}\zeta(3) + \frac{1664}{81}L_c + \mathcal{O}\left(\frac{1}{z}\right), \end{aligned} \quad (5.5)$$

$$K_{28}^{(2)\text{rem}} = K_{27}^{(1)} K_{78}^{(1)} + \left(\frac{127}{324} - \frac{35}{27}L_D\right) K_{88}^{(1)} + \frac{2}{3}(1 - L_D)K_{48}^{(1)} + \mathcal{O}\left(\frac{1}{z}\right), \quad (5.6)$$

$$K_{17}^{(2)\text{rem}} = -\frac{1}{6}K_{27}^{(2)\text{rem}} + \left(\frac{5}{16} - \frac{3}{4}L_D\right) K_{78}^{(1)} - \frac{1237}{729} + \frac{232}{27}\zeta(3) + \frac{70}{27}L_D^2 - \frac{20}{27}L_D + \mathcal{O}\left(\frac{1}{z}\right), \quad (5.7)$$

$$K_{18}^{(2)\text{rem}} = -\frac{1}{6}K_{28}^{(2)\text{rem}} + \left(\frac{5}{16} - \frac{3}{4}L_D\right) K_{88}^{(1)} + \mathcal{O}\left(\frac{1}{z}\right), \quad (5.8)$$

$$\begin{aligned} K_{77}^{(2)\text{rem}} &= \left(K_{77}^{(1)} - 4\phi_{77}^{(1)}(\delta) + \frac{2}{3}L_z\right) K_{77}^{(1)} - \frac{32}{9}L_D^2 + \frac{224}{27}L_D - \frac{628487}{729} - \frac{628}{405}\pi^4 \\ &\quad + \frac{31823}{729}\pi^2 + \frac{428}{27}\pi^2 \ln 2 + \frac{26590}{81}\zeta(3) - \frac{160}{3}L_b^2 - \frac{2720}{9}L_b + \frac{256}{27}\pi^2 L_b \\ &\quad + \frac{512}{27}\pi\alpha_{\text{Y}} + 4\phi_{77}^{(2)\text{rem}}(\delta) + \mathcal{O}\left(\frac{1}{z}\right), \end{aligned} \quad (5.9)$$

$$K_{78}^{(2)\text{rem}} = \left(-\frac{50}{3} + \frac{8}{3}\pi^2 - \frac{2}{3}L_D\right) K_{78}^{(1)} + \frac{16}{27}L_D^2 - \frac{112}{81}L_D + \frac{364}{243} + X_{78}^{(2)\text{rem}} + \mathcal{O}\left(\frac{1}{z}\right), \quad (5.10)$$

$$K_{88}^{(2)\text{rem}} = \left(-\frac{50}{3} + \frac{8}{3}\pi^2 - \frac{2}{3}L_D\right) K_{88}^{(1)} + X_{88}^{(2)\text{rem}} + \mathcal{O}\left(\frac{1}{z}\right), \quad (5.11)$$

where

$$K_{47}^{(1)\text{rem}} = K_{47}^{(1)} - \beta_0 \left(\frac{26}{81} - \frac{4}{27}L_b\right), \quad (5.12)$$

$$L_c = \ln \left(\frac{\mu_c}{m_c(\mu_c)}\right)^2, \quad (5.13)$$

and the “decoupling logarithm”

$$L_D \equiv L_b - L_z = \ln \left(\frac{\mu_b}{m_c(\mu_c)}\right)^2. \quad (5.14)$$

The function $\phi_{77}^{(2)\text{rem}}(\delta)$ reads

$$\begin{aligned} \phi_{77}^{(2)\text{rem}}(\delta) &= -4 \int_0^{1-\delta} dx \left[\frac{16}{9} F^{(2,a)} + 4 F^{(2,na)} + \frac{29}{3} F^{(2,nf)} \right] \\ &\quad - \frac{8\pi \alpha_\Upsilon}{27\delta} \left[2\delta \ln^2 \delta + (4 + 7\delta - 2\delta^2 + \delta^3) \ln \delta + 7 - \frac{8}{3}\delta - 7\delta^2 + 4\delta^3 - \frac{4}{3}\delta^4 \right], \end{aligned} \quad (5.15)$$

where $F^{(2,a)}$, $F^{(2,na)}$ and $F^{(2,nf)}$ as functions of $x = 2E_\gamma/m_b$ are given in Eqs. (7)–(9) of Ref. [8]. The terms proportional to $\alpha_\Upsilon \equiv \alpha_s^{(4)}(\mu = m_b^{1S})$ occur in Eqs. (5.9) and (5.15) because the so-called Upsilon expansion prescription [28] is followed here, which means that m_b^{pole} is expressed in terms of m_b^{1S} , and α_Υ in the ratio

$$\frac{m_b^{1S}}{m_b^{\text{pole}}} = 1 - \frac{8\pi}{9} \tilde{\alpha}_s(\mu_b) \alpha_\Upsilon + \dots \quad (5.16)$$

is treated as independent from $\tilde{\alpha}_s(\mu_b)$, i.e. it is not included in the order-counting when the $\mathcal{O}(\tilde{\alpha}_s^3(\mu_b))$ terms are neglected. A reader who wants to bypass this prescription and use another kinetic scheme for m_b should set α_Υ to zero in Eqs. (5.9) and (5.15) and at the same time replace m_b^{1S} by m_b^{pole} . Next, the latter mass should be perturbatively re-expressed in terms of the chosen m_b^{kinetic} to get rid of the renormalon ambiguity. We have verified that the $\sim 0.4\%$ effect of the α_Υ -terms on the branching ratio can be reproduced by using $m_b^{\text{pole}} = 4.74$ GeV at the considered order.

The m_c -independent quantities $X_{78}^{(2)\text{rem}}$ and $X_{88}^{(2)\text{rem}}$ in Eqs. (5.10) and (5.11) stand for the unknown non- β_0 contributions from the two-loop matrix element of Q_8 in the theory with decoupled charm (together with the corresponding bremsstrahlung). They will be set to zero in the numerical analysis. Neglecting them can be justified by arguing that the contribution of $K_{78}^{(2)}$ to $P(E_0)$ is suppressed relative to that of $K_{77}^{(2)}$ by $|Q_d C_8^{\text{eff}}/C_7^{\text{eff}}| \simeq \frac{1}{6}$. In effect, $K_{78}^{(2)\beta_0}$ in Eq. (4.6) affects $P(E_0)$ by around 0.1% only. The suppression factor gets squared for $K_{88}^{(2)}$. Thus, neglecting $X_{78}^{(2)\text{rem}}$ and $X_{88}^{(2)\text{rem}}$ is not expected to cause any significant uncertainty.

Using the results of Refs. [7,8], one easily derives an expression for the $m_c \rightarrow 0$ limit of $\tilde{K}_{77}^{(2)\text{rem}}$ that differs from $K_{77}^{(2)\text{rem}}$ by inclusion of the real $c\bar{c}$ production contributions (see Appendix B)

$$\begin{aligned} \tilde{K}_{77}^{(2)\text{rem}}(z=0) &= \left(K_{77}^{(1)} - 4\phi_{77}^{(1)}(\delta) + \frac{2}{3}L_b \right) K_{77}^{(1)} - \frac{587708}{729} + \frac{32651}{729}\pi^2 - \frac{628}{405}\pi^4 \\ &\quad + \frac{428}{27}\pi^2 \ln 2 + \frac{25150}{81}\zeta(3) - \frac{448}{9}L_b^2 + \left(\frac{80}{9}\pi^2 - \frac{2524}{9} \right) L_b \\ &\quad + \frac{512}{27}\pi\alpha_\Upsilon + 4\phi_{77}^{(2)\text{rem}}(\delta) - \frac{8\phi_{77}^{(2)\beta_0}}{3\beta_0}. \end{aligned} \quad (5.17)$$

We are going to use this formula for testing the m_c -interpolation prescription in the next section.

By analogy to Eqs. (3.14) and (4.10), we can write $P_2^{(2)\text{rem}}$ as

$$P_2^{(2)\text{rem}} \simeq \sum_{i,j=1,2,7,8} C_i^{(0)\text{eff}} C_j^{(0)\text{eff}} K_{ij}^{(2)\text{rem}}. \quad (5.18)$$

The “ \simeq ” sign is used above only because $i, j = 3, 4, 5, 6$ are skipped in the sum.

6 Interpolation in m_c

In the present section, we are going to estimate $P_2^{(2)\text{rem}}$ for $m_c < m_b/2$ by performing a certain interpolation between its large- m_c asymptotic form and an assumed value at $m_c = 0$. In particular, we shall assume that the large- β_0 approximation is accurate at $m_c = 0$, which may be argued for by recalling that no charm mass renormalization effects arise at that point. Since such an assumption is obviously a weak point of the calculation, two alternative forms of it will be considered:

$$(a) \quad P_2^{(2)\text{rem}} \xrightarrow{z \rightarrow 0} 0, \quad (6.1)$$

$$(b) \quad P_1^{(2)} + P_2^{(2)} + P_3^{(2)} \xrightarrow{z \rightarrow 0} P_2^{(2)\beta_0}. \quad (6.2)$$

The difference between these two cases will serve as a basis to estimate the interpolation uncertainty. As a cross-check, we shall also consider the case

$$(c) \quad P_2^{(2)\text{rem}} \xrightarrow{z \rightarrow 0} \left(C_7^{(0)\text{eff}}\right)^2 \widetilde{K}_{77}^{(2)\text{rem}}(z=0), \quad (6.3)$$

which does not rely on the large- β_0 approximation but rather on assuming that the “77” term dominates at $m_c = 0$. In Appendix B, issues related to the $c\bar{c}$ production are discussed.

The functional form of $P_2^{(2)\text{rem}}(z)$ that we are going to use for the interpolation is a linear combination

$$P_2^{(2)\text{rem}} = x_1 |r_2^{(1)}(z)|^2 + x_2 \text{Re } r_2^{(2)}(z) + x_3 \text{Re } r_2^{(1)}(z) + x_4 z \frac{d}{dz} \text{Re } r_2^{(1)}(z) + x_5. \quad (6.4)$$

If $P_2^{(2)\text{rem}}$ was dominated by renormalization effects, the last three terms would be sufficient. The first two terms are included because otherwise no $\ln^2 z$ would be reproduced at large z . The function $|r_2^{(1)}|^2$ is non-analytic at $m_c = m_b/2$ and takes into account the pure four-quark operator contribution to the squared amplitude. The function $\text{Re } r_2^{(2)}(z)$ matches the remaining $\ln^2 z$ in the large- m_c asymptotics. We use this function because it is the only genuine NNLO four-quark operator matrix element that is known for small z .

The determination of the coefficients x_i is most easily explained in a specific numerical example. Let us choose the renormalization scales as follows: $\mu_0 = 2M_W$, $\mu_b = m_b^{1S}/2$ and $\mu_c = m_c(m_c)$. When the central values of the input parameters from Appendix A are used but only m_c is retained arbitrary, Eq. (5.18) yields

$$P_2^{(2)\text{rem}} \simeq (9.57 + 7.12) \ln^2 z + 50.52 \ln z + 47.44 + \mathcal{O}\left(\frac{1}{z}\right), \quad (6.5)$$

where the contribution from Eq. (5.4) has been singled out in the coefficient at $\ln^2 z$ (the first term). This first term is assumed to determine x_1 . Then the second term in the coefficient at $\ln^2 z$ determines x_2 . Next, x_3 is determined from the coefficient at $\ln z$. Finally, by adjusting x_4 and x_5 , one can simultaneously match the constant term in Eq. (6.5) and satisfy

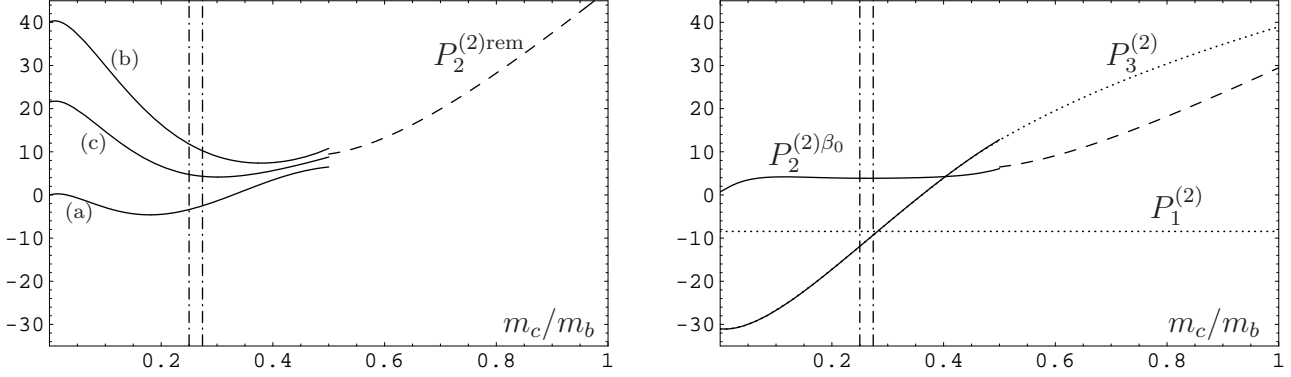


Figure 2: $P_2^{(2)\text{rem}}$, $P_2^{(2)\beta_0}$, $P_1^{(2)}$ and $P_3^{(2)}$ as functions of $m_c/m_b = \sqrt{z}$ for $\mu_0 = 2M_W$, $\mu_b = m_b^{1S}/2$ and $\mu_c = m_c(m_c)$. The other input parameters are set to their central values from Appendix A. See the text below Eq. (6.14).

one of the requirements (6.1), (6.2) or (6.3). In our example, the results are

$$\begin{aligned} \text{(a)} \quad P_2^{(2)\text{rem}}(z) &\simeq 1.45 \left[|r_2^{(1)}(z)|^2 - |r_2^{(1)}(0)|^2 \right] + 8.01 \operatorname{Re} \left[r_2^{(2)}(z) - r_2^{(2)}(0) \right] \\ &\quad + 15.63 \operatorname{Re} \left[r_2^{(1)}(z) - r_2^{(1)}(0) \right] + 16.52 z \frac{d}{dz} \operatorname{Re} r_2^{(1)}(z), \end{aligned} \quad (6.6)$$

$$\begin{aligned} \text{(b)} \quad P_2^{(2)\text{rem}}(z) &\simeq 1.45 \left[|r_2^{(1)}(z)|^2 - |r_2^{(1)}(0)|^2 \right] + 8.01 \operatorname{Re} \left[r_2^{(2)}(z) - r_2^{(2)}(0) \right] \\ &\quad + 15.63 \operatorname{Re} \left[r_2^{(1)}(z) - r_2^{(1)}(0) \right] + 0.89 z \frac{d}{dz} \operatorname{Re} r_2^{(1)}(z) + 40.15, \end{aligned} \quad (6.7)$$

$$\begin{aligned} \text{(c)} \quad P_2^{(2)\text{rem}}(z) &\simeq 1.45 \left[|r_2^{(1)}(z)|^2 - |r_2^{(1)}(0)|^2 \right] + 8.01 \operatorname{Re} \left[r_2^{(2)}(z) - r_2^{(2)}(0) \right] \\ &\quad + 15.63 \operatorname{Re} \left[r_2^{(1)}(z) - r_2^{(1)}(0) \right] + 8.14 z \frac{d}{dz} \operatorname{Re} r_2^{(1)}(z) + 21.53, \end{aligned} \quad (6.8)$$

where $P_1^{(2)} + P_3^{(2)}(z=0) \simeq -40.15$ determines the very last term in the (b) case.

Substituting the central value of $m_c(m_c)$ from Appendix A sets z to $z_0 \simeq (0.262)^2 \simeq 0.0684$. Then, $P_2^{(2)\beta_0}(z_0) \simeq 3.86$ and

$$\text{(a)} \quad P_2^{(2)\text{rem}}(z_0) \simeq -3.00 \quad \Rightarrow \quad P_2^{(2)}(z_0) \simeq 0.87, \quad (6.9)$$

$$\text{(b)} \quad P_2^{(2)\text{rem}}(z_0) \simeq 10.98 \quad \Rightarrow \quad P_2^{(2)}(z_0) \simeq 14.85, \quad (6.10)$$

$$\text{(c)} \quad P_2^{(2)\text{rem}}(z_0) \simeq 4.50 \quad \Rightarrow \quad P_2^{(2)}(z_0) \simeq 8.36. \quad (6.11)$$

The corrections $P_2^{(2)\text{rem}}$ from Eqs. (6.6), (6.7) and (6.8) are shown in the left plot of Fig. 2 as functions of $\sqrt{z} = m_c/m_b$. The other NNLO corrections $P_1^{(2)}$, $P_2^{(2)\beta_0}$ and $P_3^{(2)}$ are shown in

the right plot. For the same parameters, one finds⁶

$$P_1^{(2)} \simeq -8.45, \quad (6.12)$$

$$\begin{aligned} P_2^{(2)\beta_0}(z) &\simeq 10.35 \operatorname{Re} [r_2^{(2)}(z) - r_2^{(2)}(0)] \\ &+ 9.57 \operatorname{Re} [r_2^{(1)}(z) - r_2^{(1)}(0)] + 0.71 \quad \Rightarrow \quad P_2^{(2)\beta_0}(z_0) \simeq 3.86, \end{aligned} \quad (6.13)$$

$$P_3^{(2)}(z) \simeq 17.00 \operatorname{Re} a(z) + 16.83 \operatorname{Re} b(z) - 31.04 \quad \Rightarrow \quad P_3^{(2)}(z_0) \simeq -10.64. \quad (6.14)$$

The solid lines in Fig. 2 show the small- m_c expansions up to $\mathcal{O}(z^4)$. The dashed lines describe the leading terms in the large- m_c expansions. The dotted lines correspond to exact expressions. The (a), (b) and (c) cases of the interpolated $P_2^{(2)\text{rem}}$ are indicated in the plot. The two vertical dash-dotted lines mark the 1σ range for $m_c(m_c)/m_b^{1S}$.

As in Fig. 1, the large- and small- m_c expansions nicely match at $m_c = m_b/2$. It is only a consequence of the properties of $r_2^{(1)}$ and $\operatorname{Re} r_2^{(2)}$ that determine the z -dependence of all the considered functions.

It should be stressed that the shape of the curves in Fig. 2 is quite sensitive to the choice of renormalization scales. For instance, when the charm mass renormalization scale μ_c is shifted from its default value $\mu_c = m_c(m_c)$ to twice this value, the coefficients at $z \frac{d}{dz} \operatorname{Re} r_2^{(1)}(z)$ in Eqs. (6.6), (6.7) and (6.8) change quite dramatically (to 3.30, -12.34 and -5.09 , respectively). However, the resulting effect on the decay rate is partly compensated by a correlated change of $m_c(\mu_c)$ in the NLO correction $P_2^{(1)}$. The numerical relevance of $P_2^{(2)\beta_0}$ is very much μ_b -dependent, which compensates the μ_b -dependence of $\alpha_s(\mu_b)$ in the NLO correction. The relatively small value in Eq. (6.13) indicates that $\mu_b = m_b^{1S}/2$ that is used in this section is in the vicinity of the so-called BLM scale [29]. The renormalization scale dependence of our results will be discussed in more detail at the level of the branching ratio in the next section.

From the above results for $P_k^{(2)}$ and

$$P^{(0)} \simeq 0.1396, \quad (6.15)$$

$$P_1^{(1)} \simeq -1.515, \quad (6.16)$$

$$P_2^{(1)}(z) \simeq 3.347 - 1.826 \operatorname{Re} a(z) - 1.652 \operatorname{Re} b(z) \quad \Rightarrow \quad P_2^{(1)}(z_0) \simeq 1.151, \quad (6.17)$$

that are calculated using the same parameters, we obtain

$$(a) \quad P(E_0) \simeq 0.1226 + \mathcal{O}(\alpha_{\text{em}}, \alpha_s V_{ub}) \simeq 0.1192, \quad (6.18)$$

$$(b) \quad P(E_0) \simeq 0.1295 + \mathcal{O}(\alpha_{\text{em}}, \alpha_s V_{ub}) \simeq 0.1261, \quad (6.19)$$

$$(c) \quad P(E_0) \simeq 0.1263 + \mathcal{O}(\alpha_{\text{em}}, \alpha_s V_{ub}) \simeq 0.1229. \quad (6.20)$$

In the second step above, the electroweak and $\mathcal{O}(V_{ub})$ corrections are added according to Eq. (3.10) of Ref. [17]⁷ and Eq. (3.7) of Ref. [12], respectively.

⁶ In $P_3^{(2)}(z)$ (6.14) and $P_2^{(1)}(z)$ (6.17), we display only the z -dependence that is due to $a(z)$ and $b(z)$. Other z -dependent effects that originate from $\phi_{ij}^{(1)}(\delta)$ are very small.

⁷ We are grateful to the authors of Ref. [17] for providing us with their results in an extended version that allows for arbitrarily varying μ_0 and μ_b .

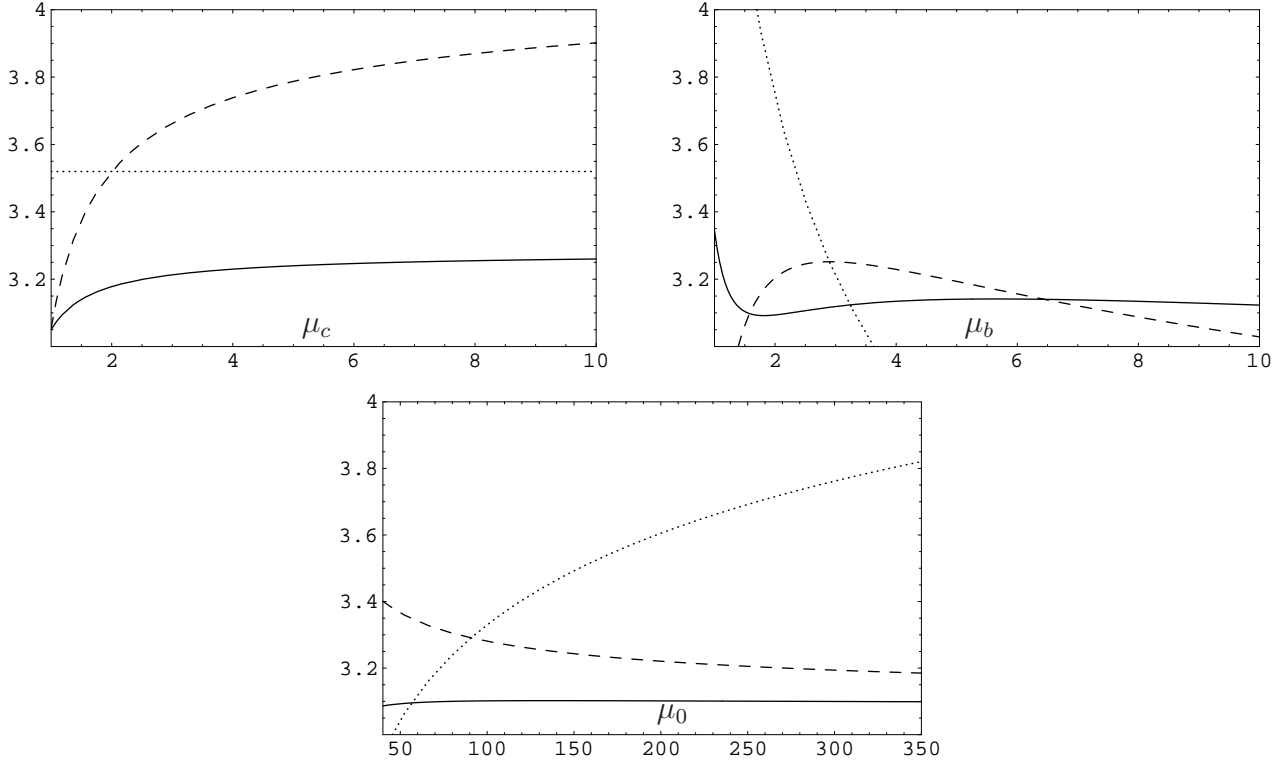


Figure 3: Renormalization scale dependence of $\mathcal{B}(\bar{B} \rightarrow X_s \gamma)$ in units 10^{-4} at the LO (dotted lines), NLO (dashed lines) and NNLO (solid lines). The upper-left, upper-right and lower plots describe the dependence on μ_c , μ_b and μ_0 [GeV], respectively.

Next, using Eq. (2.1) with $N(E_0) \simeq 0.0031$, one finds

$$(a) \quad \mathcal{B}[\bar{B} \rightarrow X_s \gamma]_{E_\gamma > 1.6 \text{ GeV}} \simeq 3.02 \times 10^{-4}, \quad (6.21)$$

$$(b) \quad \mathcal{B}[\bar{B} \rightarrow X_s \gamma]_{E_\gamma > 1.6 \text{ GeV}} \simeq 3.19 \times 10^{-4}, \quad (6.22)$$

$$(c) \quad \mathcal{B}[\bar{B} \rightarrow X_s \gamma]_{E_\gamma > 1.6 \text{ GeV}} \simeq 3.11 \times 10^{-4}. \quad (6.23)$$

7 Estimating the uncertainties

The results (a) and (b) given at the end of the previous section are within the range of around $\pm 3\%$ from their average, and the result (c) is in between them. The spread of the three solutions decreases for higher scales μ_b . Moreover, the left plot in Fig. 2 seems reasonable even as a description of an extrapolation rather than an “interpolation with an assumption”.

μ_b [GeV]	2	2.5	5	2.5	
μ_c [GeV]	1.5			$m_c(m_c)$	2.5
(a)	3.01	3.06	3.14	3.03	3.10
(b)	3.23	3.24	3.26	3.19	3.33
(c)	3.16	3.15	3.18	3.10	3.21
[(a)+(b)]/2	3.12	3.15	3.20	3.11	3.22

Table 1: $\mathcal{B}(\bar{B} \rightarrow X_s \gamma) \times 10^4$ in various cases for several choices of μ_b and μ_c . The matching scale μ_0 is set to 160 GeV, and the remaining parameters are as in Appendix A.

Therefore, we shall assign a fixed $\pm 3\%$ to the interpolation ambiguity.⁸ Unfortunately, such a rough way of determining this error may need to remain in the $\bar{B} \rightarrow X_s \gamma$ analysis until a complete evaluation of the three-loop matrix elements is performed. Calculating them just in the $m_c = 0$ case would help a lot.

As far as the higher-order ($\mathcal{O}(\alpha_s^3)$) perturbative uncertainties are concerned, renormalization-scale dependence is usually used to place lower bounds on their size. The three plots in Fig. 3 show the branching ratio dependence on each of the three scales, once the remaining two are fixed at the values that were used in the previous section ($\mu_0 = 2M_W$, $\mu_b = m_b^{1S}/2$ and $\mu_c = m_c(m_c)$). Dotted, dashed and solid lines describe the LO, NLO and NNLO results. The NNLO branching ratio is defined as the average of the (a) and (b) cases. Stabilization of the scale dependence with growing order in α_s is clearly seen. It is especially encouraging in the case of μ_b because the interpolation assumptions (6.1) and (6.2) violate the analytic μ_b -dependence cancellation even at $\mathcal{O}(\alpha_s^2)$. The μ_c -stabilization is more obvious because it is built into our interpolation prescription by construction. The perfect μ_0 -stabilization arises both due to the smaller value of α_s at the matching scale and to the fact that the NNLO matching conditions are complete.

By studying plots like those in Fig. 3 for various choices of the fixed scales, we have convinced ourselves that $\pm 3\%$ is a reasonable estimate of the higher order perturbative uncertainty. At the same time, we find that 3.15×10^{-4} is a good central value. It is reproduced (as an average of the (a) and (b) cases), e.g., for $\mu_0 = 160$ GeV, $\mu_b = 2.5$ GeV and $\mu_c = 1.5$ GeV. Table 1 contains our results for the branching ratio in various cases and for several particular choices of the renormalization scales.

The parametric uncertainty is the most straightforward one. Our input parameters and their uncertainties are listed in Appendix A. The correlation between C and $m_c(m_c)$ is taken into account. The remaining errors that are quoted in the right columns of Tables 2, 3 and 4 in Appendix A are treated as uncorrelated. This way we find the overall parametric uncertainty of $\pm 3.0\%$.

Finally, the non-perturbative uncertainties need to be considered. It has been customary for a long time to quote the known $\mathcal{O}(\Lambda^2/m_b^2)$ and $\mathcal{O}(\Lambda^2/m_c^2)$ non-perturbative corrections as the

⁸ Various uncertainties will be added in quadrature later. Thus, each of them should be understood as a “theoretical 1σ ” rather than a strict range. Of course, such statements concerning theoretical uncertainties are never well-defined, but one can hardly improve on this point.

dominant ones (see Section VI of Ref. [30] for discussion and references). The subdominant $\mathcal{O}(\Lambda^2/m_b^3)$ and $\mathcal{O}(\Lambda^2/(m_c^2 m_b))$ ones are known, too [13]. More recently, the $\mathcal{O}(\alpha_s \Lambda^2/(m_b - 2E_0)^2)$ correction was evaluated [14]. All these corrections are included in $N(E_0)$ in Eq. (2.1) and cause around 2.4% enhancement of the branching ratio. However, the non-perturbative corrections that arise in the matrix elements of $Q_{1,2}$ in the presence of one gluon that is not soft remain unknown. They scale like $\alpha_s \Lambda/m_b$ in the limit $m_c \ll m_b/2$ and like $\alpha_s \Lambda^2/m_c^2$ in the limit $m_c \gg m_b/2$.⁹ Since $m_c < m_b/2$ in reality, we consider $\alpha_s \Lambda/m_b$ as the quantity that sets the size of such effects. In consequence, we assign a $\pm 5\%$ non-perturbative uncertainty to our result. This is the dominant uncertainty at the moment. The very recent estimates [31] of similar corrections to the Q_7 - Q_8 interference term are neglected here. They are smaller than the overall uncertainty of $\pm 5\%$ that both the authors of Ref. [31] and us assign to *all* the unknown $\mathcal{O}(\alpha_s \Lambda/m_b)$ effects.

8 Conclusions

Our final NNLO result

$$\mathcal{B}[\bar{B} \rightarrow X_s \gamma]_{E_\gamma > 1.6 \text{ GeV}} \simeq (3.15 \pm 0.23) \times 10^{-4} \quad (8.1)$$

is obtained for the input parameters listed in Appendix A and for the renormalization scales $\mu_0 = 160 \text{ GeV}$, $\mu_b = 2.5 \text{ GeV}$ and $\mu_c = 1.5 \text{ GeV}$. The total uncertainty is found by combining in quadrature the ones discussed in Section 7. As it is clearly seen in Fig. 3, the NNLO corrections significantly improve the stability of the prediction with respect to the renormalization scale variation and, in consequence, reduce the total error. Comparing the NLO and NNLO μ_c -dependence in Fig. 3, one realizes why all the previously published NLO predictions had significantly higher central values than the current NNLO one.

In order to relate our result with $E_0 = 1.6 \text{ GeV}$ to the measurements with cuts at 1.8 GeV (Belle [32]) and 1.9 GeV (BaBar [33]), one needs to compute ratios of the decay rates with different cuts (see, e.g., Ref. [34]). This is a non-trivial issue because new perturbative and non-perturbative effects become important in the endpoint region. A new calculation of such effects has recently been completed [35] but its numerical results were not yet available when the average in Eq. (1.1) was being evaluated.

We have chosen $E_0 = 1.6 \text{ GeV}$ as default here assuming that it is low enough for the cutoff-enhanced perturbative corrections [14, 35] to become negligible. If this turns out not to be the case, one should use our results with lower E_0 . For this purpose, we give¹⁰

$$\mathcal{B}[\bar{B} \rightarrow X_s \gamma]_{E_\gamma > 1.5 \text{ GeV}} \simeq (3.18 \pm 0.23) \times 10^{-4}, \quad (8.2)$$

$$\mathcal{B}[\bar{B} \rightarrow X_s \gamma]_{E_\gamma > 1.4 \text{ GeV}} \simeq (3.20 \pm 0.23) \times 10^{-4}, \quad (8.3)$$

$$\mathcal{B}[\bar{B} \rightarrow X_s \gamma]_{E_\gamma > 1.3 \text{ GeV}} \simeq (3.22 \pm 0.23) \times 10^{-4}, \quad (8.4)$$

⁹ We thank M. Beneke for a clarifying discussion on this point.

¹⁰ These results do not include contributions from tree-level diagrams with four quark operator insertions that are suppressed either by $|V_{ub}|^2$ or by squares of the small Wilson coefficients C_3, \dots, C_6 [27].

$$\mathcal{B}[\bar{B} \rightarrow X_s \gamma]_{E_\gamma > 1.2 \text{ GeV}} \simeq (3.24 \pm 0.23) \times 10^{-4}, \quad (8.5)$$

$$\mathcal{B}[\bar{B} \rightarrow X_s \gamma]_{E_\gamma > 1.1 \text{ GeV}} \simeq (3.25 \pm 0.23) \times 10^{-4}, \quad (8.6)$$

$$\mathcal{B}[\bar{B} \rightarrow X_s \gamma]_{E_\gamma > 1.0 \text{ GeV}} \simeq (3.27 \pm 0.23) \times 10^{-4}. \quad (8.7)$$

Note added

A numerical analysis of cutoff-related perturbative corrections (see Section 8) became available [36] when the current paper was being refereed. The authors of Ref. [36] use our result given in Eq. (8.7) and combine it with their cutoff-related corrections that turn out to suppress the branching ratio at $E_0 = 1.6 \text{ GeV}$ by around 3% with respect to Eq. (8.1). Such an effect is of the same size as our higher-order uncertainty, which means that the unknown $O(\alpha_s^3)$ non-logarithmic effects can be as important at $E_0 = 1.6 \text{ GeV}$ as the logarithmic ones calculated in Ref. [36]. Therefore, we leave the results of the current paper unaltered, yet not excluding the possibility of taking the correction from Ref. [36] into account in future upgrades of the phenomenological analysis, once other effects of potentially the same size are collected (see Section 1 of Ref. [37]).

Acknowledgments

We would like to thank Aneesh Manohar for information on correlations among parameters that are determined in the global semileptonic fit in Refs. [38–40]. We are grateful to Paolo Gambino and Ulrich Haisch for cross-checking the numerical results for $P_3^{(2)}$ and $P_1^{(2)}$, respectively, as well as for their help concerning the $\mathcal{O}(\Lambda^3)$ and electroweak corrections. This work was supported in part by the EU Contract MRTN-CT-2006-035482, FLAVIANet. M.M. acknowledges support by the Polish Committee for Scientific Research under the grant 2 P03B 078 26, and from the EU Contract HPRN-CT-2002-00311, EURIDICE. M.S. acknowledges support by the DFG through SFB/TR 9.

Appendix A: Numerical inputs

In this appendix, we collect numerical parameters that are used in Sections 6 and 7. The default value of the photon energy cut is $E_0 = 1.6 \text{ GeV}$. In Section 6, the renormalization scales were $\mu_0 = 2M_W$, $\mu_b = m_b^{1S}/2$ and $\mu_c = m_c(m_c)$. The final central value of the branching ratio in Eq. (8.1) is reproduced e.g. for $\mu_0 = 160 \text{ GeV}$, $\mu_b = 2.5 \text{ GeV}$ and $\mu_c = 1.5 \text{ GeV}$.

The other parameters are displayed in the tables below. Errors are indicated only if varying a given parameter within its 1σ range causes a larger than $\pm 0.1\%$ effect on the branching ratio (8.1). In such cases, the effects in percent are given in the right column of the corresponding table.

Table 2 contains the four quantities that determine the overall normalization factor multiplying $P(E_0)$ in the expression (2.1) for the branching ratio.

parameter	effect on Eq. (8.1)
$\mathcal{B}(B \rightarrow X_c e \bar{\nu})_{\text{exp}} = 0.1061 \pm 0.0017$ [42]	$\pm 1.6\%$
$C = 0.580 \pm 0.016$ [39, 41]	$\pm 2.8\%$
$ V_{ts}^* V_{tb}/V_{cb} ^2 = 0.9676 \pm 0.0033$ [43, 44]	$\pm 0.4\%$
$\alpha_{\text{em}}(0) = 1/137.036$ [45]	

Table 2: Parameters that determine the overall normalization factor in Eq. (2.1).

parameter	effect on Eq. (8.1)
$M_Z = 91.1876$ GeV [45]	
$\alpha_s(M_Z) = 0.1189 \pm 0.0020$ [45, 46]	$\pm 2.0\%$
$m_{t,\text{pole}} = (171.4 \pm 2.1)$ GeV [47]	$\pm 0.5\%$
$M_W = 80.403$ GeV [45]	
$m_b^{1S} = (4.68 \pm 0.03)$ GeV [39]	$\pm 0.2\%$
$m_c(m_c) = (1.224 \pm 0.017 \pm 0.054)$ GeV [40]	$\pm 2.8\%$

Table 3: Experimental inputs that are necessary in the calculation of $P(E_0)$ before including the electroweak and $\mathcal{O}(V_{ub})$ corrections.

Table 3 contains the experimental inputs that are necessary in the calculation of $P(E_0)$, before including the electroweak and $\mathcal{O}(V_{ub})$ corrections. For $\alpha_s(M_Z)$, we adopt the central value from Ref. [46] but conservatively use a twice larger error which then overlaps with the one given by the PDG [45]. One should take into account that the phase space factor C in Table 2 and $m_c(m_c)$ in Table 3 are strongly correlated. For this reason, we take both parameters as determined in the same global fit to the semileptonic B -decay spectra [38–40] instead of adopting $m_c(m_c)$ from Ref. [48]. The normalized correlation coefficient amounts to [41]

$$F \equiv \frac{\langle C m_c \rangle - \langle C \rangle \langle m_c \rangle}{\sigma_C \sigma_{m_c}} \simeq \begin{cases} -0.97, & \text{method A,} \\ -0.92, & \text{method B,} \end{cases} \quad (\text{A.1})$$

where the meaning of the two methods is explained in Section III of Ref. [40]. Denoting the uncertainties in the right columns of Tables 2 and 3 by Δ_x , where x is the relevant variable, one finds that the combined uncertainty due to C and m_c is given by

$$\Delta_{C,m_c} = \sqrt{\Delta_C^2 + \Delta_{m_c}^2 + 2F|\Delta_C \Delta_{m_c}|}. \quad (\text{A.2})$$

Since Δ_C and Δ_{m_c} are very close in size (by coincidence) and F is close to -1 , the combined uncertainty is much smaller than it would be in the absence of the correlation. For our final result, we adopt $F = -0.92$ that gives larger Δ_{C,m_c} ($\pm 1.1\%$ rather than $\pm 0.7\%$).

The dependence of $m_c(m_c)$ on $\alpha_s(M_Z)$ in the semileptonic fit can affect $m_c(m_c)$ by up to ~ 10 MeV [41], which would translate to $\sim 0.5\%$ in Δ_{α_s} . We neglect this effect here. An analogous correlation for C is also neglected, as it turns out to be even smaller [41].

parameter	effect on Eq. (8.1)
$\alpha_{\text{em}}(M_Z) = 1/128.940$ [49, 50] $\sin^2 \theta_W = 0.2324$ [51] $M_{\text{Higgs}} \in [114.4, 194] \text{ GeV}$ (95% C.L) [45] (115 GeV is used as central) $(V_{us}^* V_{ub}) / (V_{ts}^* V_{tb}) = -0.011 + 0.018i$ [43, 44] $\lambda_1 = (-0.27 \pm 0.04) \text{ GeV}^2$ [39] $\lambda_2 \simeq \frac{1}{4} (m_{B^*}^2 - m_B^2) \simeq 0.12 \text{ GeV}^2$ [45] $\rho_1 = (0.038 \pm 0.028) \text{ GeV}^3$ [39, 41] $\rho_2 = (0.0045 \pm 0.035) \text{ GeV}^3$ [39, 41]	0.3% $\pm 0.4\%$ $\pm 0.6\%$

Table 4: Remaining parameters that are necessary for the electroweak, $\mathcal{O}(V_{ub})$ and non-perturbative corrections.

i	$C_i^{(0)\text{eff}}(\mu_b)$	$C_i^{(1)\text{eff}}(\mu_b)$
1	-0.8411	15.278
2	1.0647	-2.124
3	-0.0133	0.096
4	-0.1276	-0.463
5	0.0012	-0.021
6	0.0028	-0.013
7	-0.3736	2.027
8	-0.1729	-0.614

Table 5: The LO and NLO Wilson coefficients $C_i^{(k)\text{eff}}(\mu_b)$ at $\mu_b = m_b^{1S}/2 = 2.34 \text{ GeV}$. The matching scale μ_0 was set to $2M_W$ in their evaluation.

Table 4 contains the remaining parameters that are necessary for the electroweak, $\mathcal{O}(V_{ub})$ and non-perturbative corrections. Since we treat the phase space factor C as an independent input, λ_1 is needed only for the small cutoff-related non-perturbative correction [14].

The parameters ρ_1 and ρ_2 are needed for the $\mathcal{O}(\Lambda^3/m_b^3, \Lambda^3/(m_b m_c^2))$ contributions to $N(E_0)$ that are derived from the formulae of Refs. [13, 52]. An important subtlety in this calculation is that the $\mathcal{O}(\Lambda^3/m_b^3)$ corrections to $\Gamma(\bar{B} \rightarrow X_u e \nu)$ logarithmically diverge when $m_u \rightarrow 0$, so long as hard gluon interactions with the spectator quark are neglected. When they are included, one encounters new non-perturbative matrix elements whose values are rather uncertain [53]. Since these effects cancel in the ratio $(P(E_0) + N(E_0))/C$, we follow the approach that has been used in the calculation of C in Ref. [39], namely we neglect the spectator effects and set $\ln m_b/m_u$ to zero. At the same time, we neglect the additional uncertainty in C that is caused by this arbitrary procedure (see the comments below Eq. (25) in Ref. [39]). Our final result (8.1) is the same as if the considered subtlety did not occur at all. In the future, simultaneous

calculations of C and $N(E_0)$ should be performed on the basis of the semileptonic fit results of Ref. [34], which would constitute an independent test of the the current calculation.

Although the Wilson coefficients $C_i^{\text{eff}}(\mu_b)$ are derived quantities, we quote for convenience their values at $\mu_b = m_b^{1S}/2$. The LO and NLO ones are collected in Table 5. From among the NNLO ones, only $C_7^{(2)\text{eff}}(\mu_b)$ is relevant here. We find $C_7^{(2)\text{eff}}(m_b^{1S}/2) \simeq 16.81$ including the four-loop mixing $(Q_1, \dots, Q_6) \rightarrow Q_7$ but neglecting the four-loop mixing $(Q_1, \dots, Q_6) \rightarrow Q_8$.

The analytical solutions to the NNLO RGE for the Wilson coefficients can be found, e.g., in Section 3.3 of Ref. [54]. The resulting explicit expressions for $C_i^{(k)\text{eff}}(\mu_b)$ in terms of $C_i^{(k)\text{eff}}(\mu_0)$ and $\eta = \alpha_s(\mu_0)/\alpha_s(\mu_b)$ are given in Ref. [6]. As far as $\alpha_s(\mu)$ is concerned, we have used the four-loop RGE and applied two independent methods for solving it: a numerical one implemented in `RunDec` [55] and an iterative analytical one that includes (tiny) QED effects, too [54]. Our final results are independent of which method is used. However, the intermediate quantities, for which more digits are presented, slightly depend on the method.

Appendix B: The $m_c = 0$ case and $c\bar{c}$ production

The $\bar{B} \rightarrow X_s \gamma$ branching ratio contains no contribution from $c\bar{c}$ production because events involving charmed hadrons in the final state are not included on the experimental side. Thus, the evaluation of $b \rightarrow X_s^{\text{parton}} \gamma$ should be performed accordingly. However, such a definition of $b \rightarrow X_s^{\text{parton}} \gamma$ may break down for $m_c \rightarrow 0$, since logarithmic divergences containing $\ln m_c$ may arise in $P_2^{(2)\text{rem}}$.

No such divergences are present in the NLO contributions to $P(E_0)$, and in the other than $P_2^{(2)\text{rem}}$ NNLO ones. There, all the logarithms of m_c get multiplied by positive powers of this mass. If $P_2^{(2)\text{rem}}$ turns out to be logarithmically divergent at $m_c \rightarrow 0$, it should be redefined to include the $c\bar{c}$ production contributions. The assumptions (6.1)–(6.3) would then refer to the redefined quantity that must be convergent at $m_c \rightarrow 0$. At the same time, the large- m_c asymptotics would remain unaltered. After performing the interpolation of the redefined quantity as in Section 6, one should subtract the $c\bar{c}$ production effects at the measured value of m_c . At present, possible effects of such a subtraction are understood to be contained in the interpolation ambiguity.

Actually, Eq. (5.17) does contain the $c\bar{c}$ production contributions in the $m_c \rightarrow 0$ case. However, it is used only in the assumption (6.3) that serves just as a cross check, and has no influence on our final numerical result (8.1).

References

- [1] E. Barberio *et al.*, (Heavy Flavor Averaging Group), hep-ex/0603003.
- [2] C. Bobeth, M. Misiak and J. Urban, Nucl. Phys. B **574** (2000) 291 [hep-ph/9910220].
- [3] M. Misiak and M. Steinhauser, Nucl. Phys. B **683** (2004) 277 [hep-ph/0401041].
- [4] M. Gorbahn and U. Haisch, Nucl. Phys. B **713** (2005) 291 [hep-ph/0411071].

- [5] M. Gorbahn, U. Haisch and M. Misiak, Phys. Rev. Lett. **95** (2005) 102004 [hep-ph/0504194].
- [6] M. Czakon, U. Haisch and M. Misiak, hep-ph/0612329.
- [7] I. Blokland, A. Czarnecki, M. Misiak, M. Ślusarczyk and F. Tkachov, Phys. Rev. D **72** (2005) 033014 [hep-ph/0506055].
- [8] K. Melnikov and A. Mitov, Phys. Lett. B **620** (2005) 69 [hep-ph/0505097].
- [9] H. M. Asatrian, A. Hovhannisyan, V. Poghosyan, T. Ewerth, C. Greub and T. Hurth, Nucl. Phys. B **749** (2006) 325 [hep-ph/0605009].
- [10] H. M. Asatrian, T. Ewerth, A. Ferroglia, P. Gambino and C. Greub, hep-ph/0607316.
- [11] K. Bieri, C. Greub and M. Steinhauser, Phys. Rev. D **67** (2003) 114019 [hep-ph/0302051].
- [12] P. Gambino and M. Misiak, Nucl. Phys. B **611** (2001) 338 [hep-ph/0104034].
- [13] C. W. Bauer, Phys. Rev. D **57** (1998) 5611, Phys. Rev. D **60** (1999) 099907 (E) [hep-ph/9710513].
- [14] M. Neubert, Eur. Phys. J. C **40** (2005) 165 [hep-ph/0408179].
- [15] T. van Ritbergen, Phys. Lett. B **454** (1999) 353 [hep-ph/9903226].
- [16] T. Seidensticker and M. Steinhauser, Phys. Lett. B **467** (1999) 271 [hep-ph/9909436].
- [17] P. Gambino and U. Haisch, JHEP **0110** (2001) 020, [hep-ph/0109058].
- [18] A.J. Buras, M. Misiak, M. Münz and S. Pokorski, Nucl. Phys. B **424** (1994) 374 [hep-ph/9311345].
- [19] K.G. Chetyrkin, M. Misiak and M. Münz, Phys. Lett. B **400** (1997) 206, Phys. Lett. B **425** (1998) 414 (E) [hep-ph/9612313].
- [20] A.J. Buras, A. Czarnecki, M. Misiak and J. Urban, Nucl. Phys. B **631** (2002) 219 [hep-ph/0203135].
- [21] A. H. Hoang, Phys. Rev. D **61** (2000) 034005 [hep-ph/9905550].
- [22] C. Greub, T. Hurth and D. Wyler, Phys. Rev. D **54** (1996) 3350 [hep-ph/9603404].
- [23] A. J. Buras, A. Czarnecki, M. Misiak and J. Urban, Nucl. Phys. B **611** (2001) 488 [hep-ph/0105160].
- [24] N. Pott, Phys. Rev. D **54** (1996) 938 [hep-ph/9512252].
- [25] M. Steinhauser, Comput. Phys. Commun. **134** (2001) 335 [hep-ph/0009029].

- [26] M. Misiak and M. Steinhauser, in preparation.
- [27] Z. Ligeti, M.E. Luke, A.V. Manohar and M.B. Wise, Phys. Rev. D **60** (1999) 034019 [hep-ph/9903305].
- [28] A. H. Hoang, Z. Ligeti and A. V. Manohar, Phys. Rev. D **59** (1999) 074017 [hep-ph/9811239].
- [29] S. J. Brodsky, G. P. Lepage and P. B. Mackenzie, Phys. Rev. D **28** (1983) 228.
- [30] T. Hurth, Rev. Mod. Phys. **75** (2003) 1159 [hep-ph/0212304].
- [31] S. J. Lee, M. Neubert and G. Paz, hep-ph/0609224.
- [32] P. Koppenburg *et al.* (Belle Collaboration), Phys. Rev. Lett. **93** (2004) 061803 [hep-ex/0403004].
- [33] B. Aubert *et al.* (BaBar Collaboration), hep-ex/0607071;
B. Aubert *et al.* (BaBar Collaboration), Phys. Rev. D **72** (2005) 052004 [hep-ex/0508004].
- [34] O. Buchmüller and H. Flächer, Phys. Rev. D **73** (2006) 073008 [hep-ph/0507253].
- [35] T. Becher and M. Neubert, Phys. Lett. B **633** (2006) 739 [hep-ph/0512208], Phys. Lett. B **637** (2006) 251 [hep-ph/0603140].
- [36] T. Becher and M. Neubert, hep-ph/0610067.
- [37] H. M. Asatrian, T. Ewerth, H. Gabrielyan and C. Greub, hep-ph/0611123.
- [38] C. W. Bauer, Z. Ligeti, M. Luke and A. V. Manohar, Phys. Rev. D **67** (2003) 054012 [hep-ph/0210027].
- [39] C. W. Bauer, Z. Ligeti, M. Luke, A. V. Manohar and M. Trott, Phys. Rev. D **70** (2004) 094017 [hep-ph/0408002].
- [40] A. H. Hoang and A. V. Manohar, Phys. Lett. B **633** (2006) 526 [hep-ph/0509195].
- [41] A. V. Manohar, private communication.
- [42] B. Aubert *et al.* (BaBar Collaboration), Phys. Rev. Lett. **93**, 011803 (2004) [hep-ex/0404017].
- [43] M. Bona *et al.* (UTfit Collaboration), JHEP **0610** (2006) 081 [hep-ph/0606167].
- [44] J. Charles *et al.* (CKMfitter Group), Eur. Phys. J. C **41**, 1 (2005) [hep-ph/0406184], <http://www.slac.stanford.edu/xorg/ckmfitter>.
- [45] W. M. Yao *et al.* (Particle Data Group), J. Phys. G **33** (2006) 1.
- [46] S. Bethke, hep-ex/0606035.

- [47] Tevatron Electroweak Working Group, hep-ex/0608032.
- [48] J. H. Kühn and M. Steinhauser, Nucl. Phys. B **619** (2001) 588, Nucl. Phys. B **640** (2002) 415 (E) [hep-ph/0109084].
- [49] J. H. Kühn and M. Steinhauser, Phys. Lett. B **437** (1998) 425 [hep-ph/9802241].
- [50] H. Burkhardt and B. Pietrzyk, Phys. Rev. D **72** (2005) 057501 [hep-ph/0506323].
- [51] The LEP Electroweak Working Group, <http://lepewwg.web.cern.ch/LEPEWWG> .
- [52] M. Gremm and A. Kapustin, Phys. Rev. D **55** (1997) 6924 [hep-ph/9603448].
- [53] P. Gambino, G. Ossola and N. Uraltsev, JHEP **0509** (2005) 010 [hep-ph/0505091].
- [54] T. Huber, E. Lunghi, M. Misiak and D. Wyler, Nucl. Phys. B **740** (2006) 105 [hep-ph/0512066].
- [55] K. G. Chetyrkin, J. H. Kuhn and M. Steinhauser, Comput. Phys. Commun. **133** (2000) 43 [hep-ph/0004189].